Supporting Information for "Dune geometry and the associated hydraulic roughness at the transition from a fluvial to tidal regime at low river discharge"

S.I. de Lange[1], R. Bradley[2,3], R.A. Schrijvershof [1], D. Murphy[3], K. Waldschläger[1], R. Kostaschuk[3], J.G. Venditti[3], A.J.F. Hoitink[1]

[1]Wageningen University, Department of Environmental Sciences, Hydrology and Quantitative Water Management, Wageningen, the Netherlands

[2]Northwest Hydraulic Consultants Ltd., North Vancouver, British Columbia, Canada

[3]School of Environmental Science, Simon Fraser University, Burnaby, British Columbia, Canada

Contents of this file

Introduction In these supplementary materials, six topics will be discussed and/or visualised. These include surface geology of the lower Fraser river, examples of bathymetric data where (human-made) irregularities are visible, the model calibration and evaluation, figures visualising the predictive capacity for dune patterns of several dune height predictors, some additional figures on the local focus areas, and a figure indicating the intertidal areas.

Text S1: Surface geology The surface geology (Figure S1) determines the underlying material of the Fraser river, and is often exposed on the channel margin. At the outer banks of the river, gravel and clay patches are present (Figure 2a and c). These patches of gravel and clay are either caused by modern deposits, such as gravel bars, or by earlier deposited sediments constraining the river's course. When the river cuts into a clay or gravel layer, abrupt changes in dune geometry can be visible.

Text S2: Examples of bathymetric data with (human-made) irregularities

see Figure S2

Text S3: Model calibration and evaluation

The model was calibrated by assessing the tidal amplitude of the M_2, M_4 and K_1 tidal constituents, during low water levels in winter 2018. A uniform roughness of 0.026 s $m^{-1/3}$ performs the best. The performance of best performing model, and the other tests using different values of uniform roughness, are summarized in Table S2, indicating the Root Mean Square Error of the observed and modelled water level (between 0.27 and 0.43 m), the correlation coefficient R^2 between the observed and modelled water level (between 0.67 and 0.87), and the difference in observed and modelled tidal amplitude of the M2, K1 and M4 tidal constituents (observed divided by modelled values), with a maximum over/under estimation of 5%, 6% and 390%, respectively).

When implementing a roughness break at the regime change and testing various roughness values before and after the regime change, the calibration can improve slightly for certain parameters at certain stations (Figure S3a). However, there is no model that performs better in all aspects than the uniform roughness model (Table S1).

When implementing dune-adjusted roughness, the calibration does not improve (Figure S3b and Table S2). When using 1/2 k_s in equation 2, following the suggestion of Davies and Robins (2017) that the total effective hydraulic roughness is half of the dune

roughness, the dune roughness corresponds well with the calibrated model roughness in the mixed fluvial-tidal regime (RK > 40) (Figure S4).

Text S4: Dune height prediction see Figure S5 and S6

Text S5: Additional information on focus zones see Figure S7 , S8, S9 and S10

Text S6: Intertidal areas see Figure S11

References

Davies, A. G., & Robins, P. E. (2017). Residual flow, bedforms and sediment transport in a tidal channel modelled with variable bed roughness. *Geomorphology*, *295*, 855–872. Retrieved from `http://dx.doi.org/10.1016/j.geomorph.2017.08.029` doi: 10.1016/j.geomorph.2017.08.029

Turner, R., Clague, J., Groulx, B., & Journeay, J. (1998). *GeoMap Vancouver, geological map of the Vancouver Metropolitan area.* Geological Survey of Canada, Open File 3511, 1998, 1 sheet. doi: https://doi.org/10.4095/209909

Van Rijn, L. (1984). Sediment transport, part III: Bedforms. *Journal of Hydraulic Engineering*, *110*(12), 1733–1754.

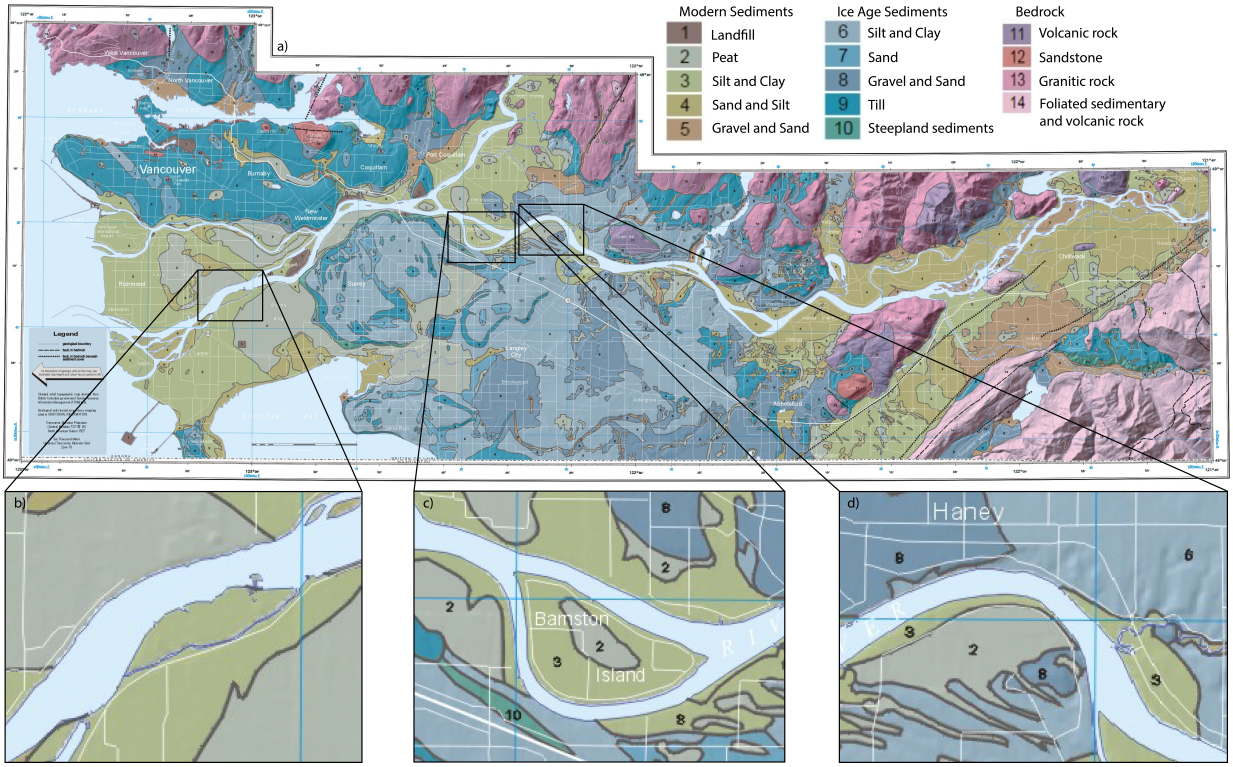

Figure S1. Surficial geology map (a), zoomed in on the focus areas (b, c, d). Adjusted from Turner et al. (1998).

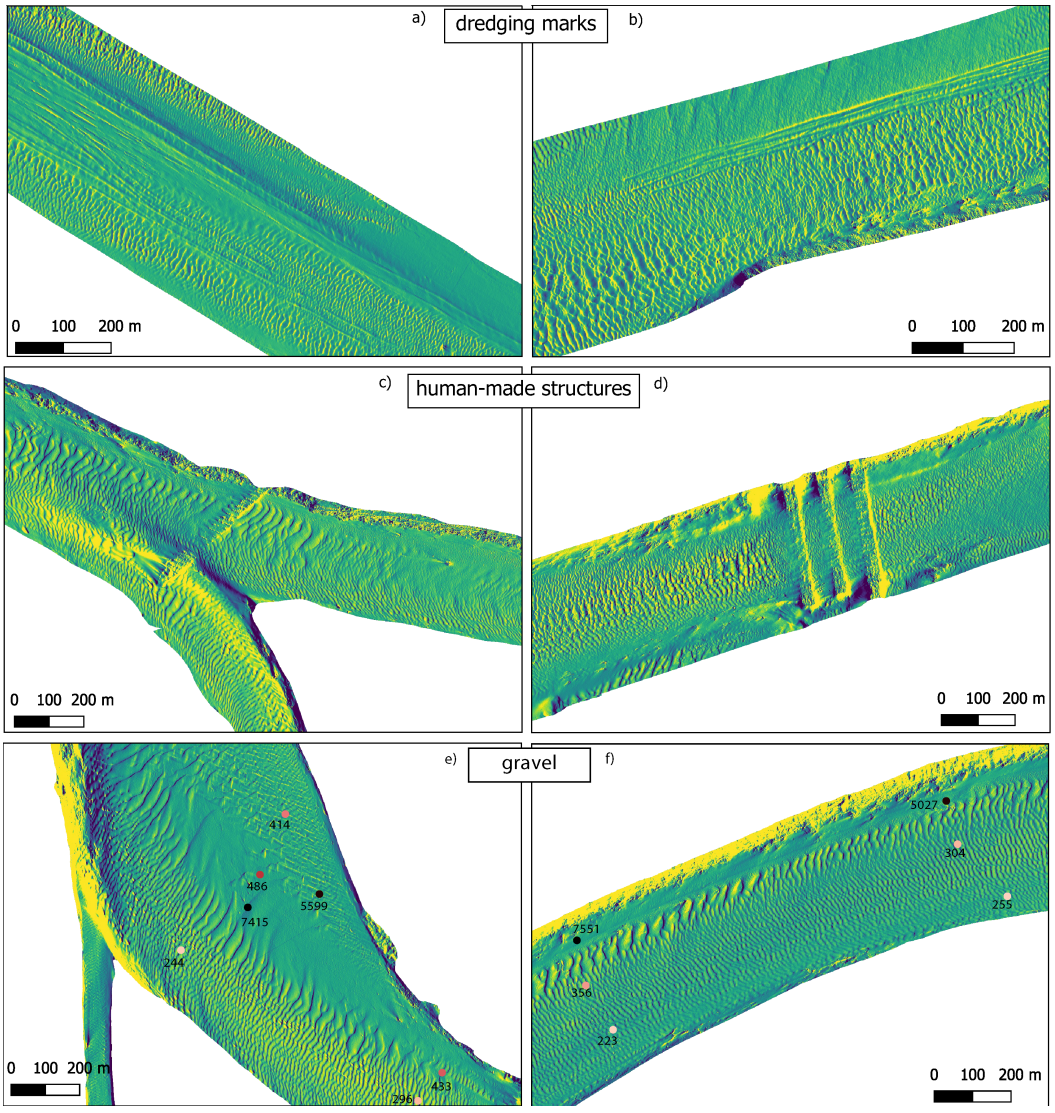

Figure S2. Example of bathymetric data with a, b) dredging marks, c, d) human-made structures e, f) gravel deposits, featuring no dunes. Median grain size (μm) is indicated.

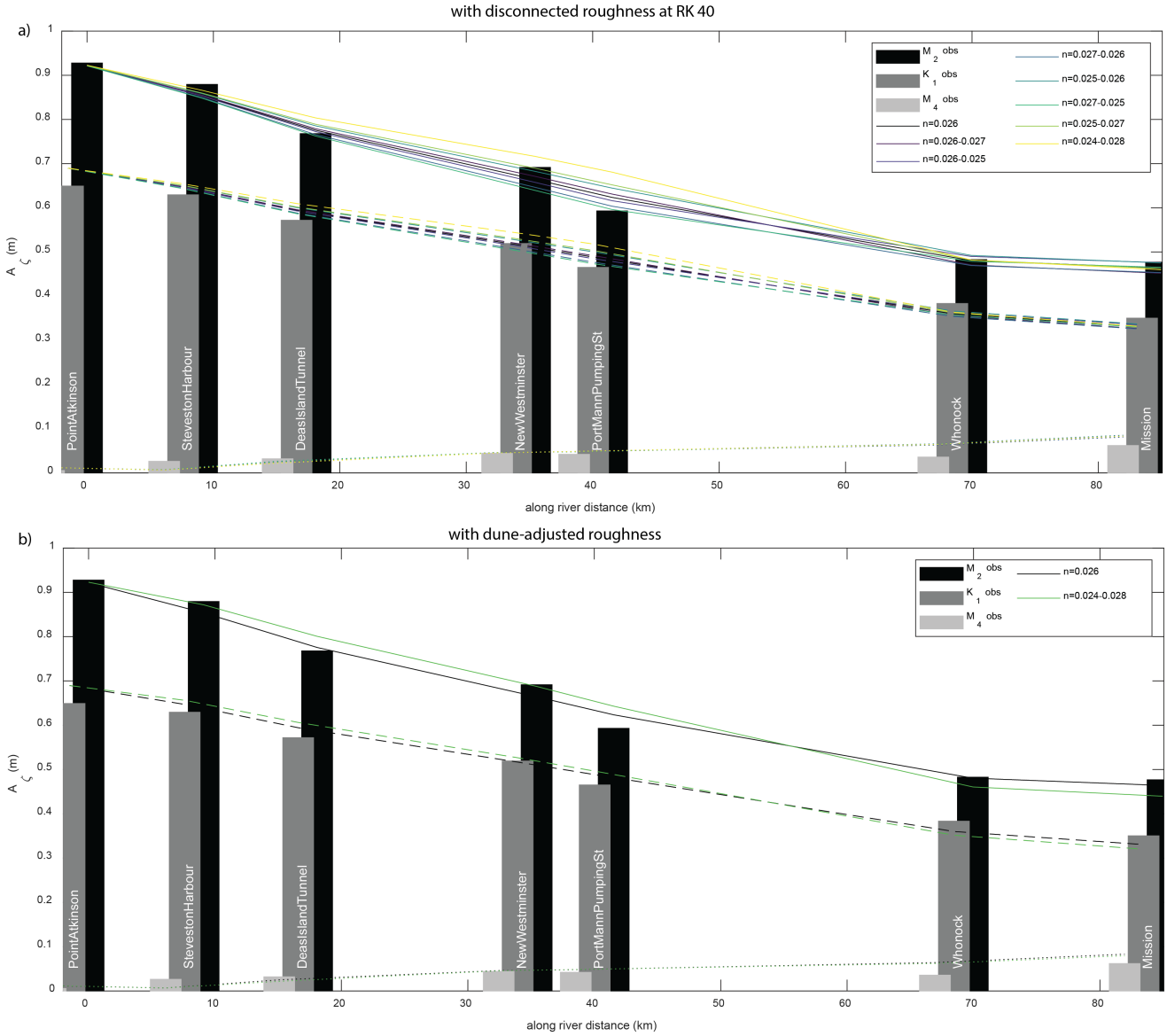

Figure S3. Performance of the model, with a disconnected roughness at the regime change at RK 40 (a) and dune-adjusted roughness (b). The observed tidal amplitude of the tidal constituents M2 (black bars), K1 (dark grey bars), and M4 (light grey bars) are indicated by bars, and the corresponding modelled tidal amplitudes for the various models are indicated with lines.

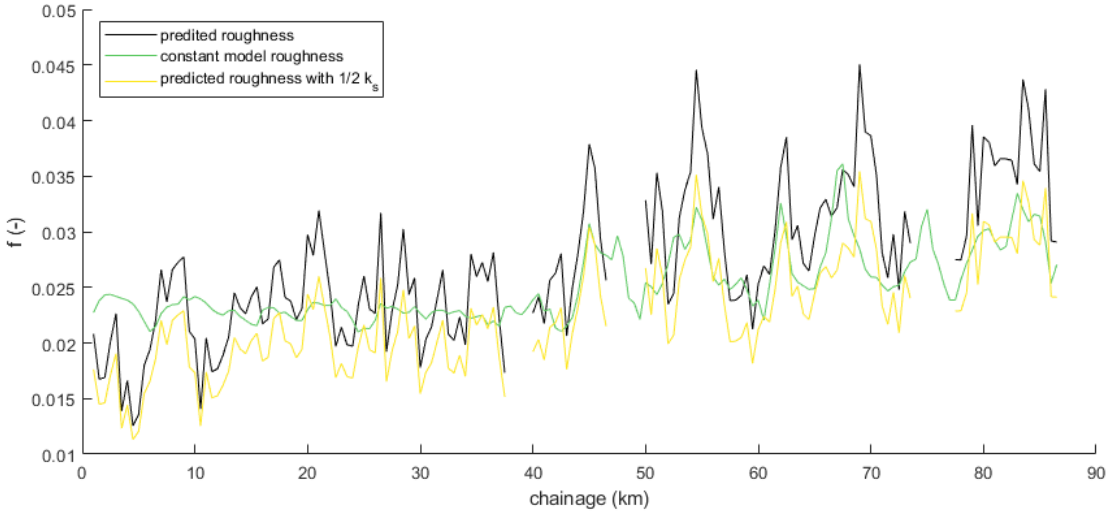

Figure S4. Hydraulic roughness in the study area expressed in f. Roughness calculated from dune geometry (equation13 in main manuscript)(black), model roughness with a constant Manning's n of 0.026 s $m^{-1/3}$ (green) and roughness calculated from dune geometry, using 1/2 k_s.

Table S1. Model evaluation of the model with uniform roughness (n_{man}=0.026) and a roughness break at RK 40, allowing two constant roughness value downstream and upstream of this break. The models are evaluated with the Root Mean Square Error (RMSE) of the observed and modelled water level (h), and the difference in observed and modelled tidal amplitude (Aζ) of the M2, K1 and M4 tidal constituents (observed divided by modelled values). The mean of the latter is calculated as the absolute values of Aζ - 1.

	Roughness model	Point Atkinson	Steveston Harbour	Deas Island Tunnel	New Westminster	Port Mann Pumping St	Whonock	Mission	Mean all stations
	0.026	0.341	0.363	0.346	0.430	0.380	0.305	0.266	0.347
	0.026-0.027	0.341	0.363	0.347	0.431	0.379	0.306	0.270	0.348
	0.026-0.025	0.341	0.362	0.345	0.429	0.381	0.305	0.264	0.347
	0.027-0.026	0.340	0.363	0.344	0.422	0.377	0.306	0.267	0.346
	0.025-0.026	0.341	0.363	0.348	0.439	0.385	0.305	0.265	0.349
	0.027-0.025	0.340	0.362	0.344	0.421	0.378	0.305	0.265	0.345
	0.025-0.027	0.341	0.364	0.348	0.439	0.384	0.305	0.269	0.350
RMSE h (m)	0.024-0.028	0.341	0.365	0.351	0.449	0.388	0.305	0.273	0.353
	0.026	1.01	1.03	0.99	1.04	0.95	1.00	1.03	0.024
	0.026-0.027	1.01	1.03	0.99	1.03	0.94	1.03	1.06	0.031
	0.026-0.025	1.01	1.03	0.99	1.05	0.96	0.99	1.00	0.021
	0.027-0.026	1.01	1.04	1.00	1.07	0.98	1.03	1.05	0.030
	0.025-0.026	1.01	1.02	0.98	1.01	0.92	0.98	1.00	0.024
	0.027-0.025	1.01	1.04	1.01	1.08	0.99	1.01	1.02	0.024
	0.025-0.027	1.01	1.02	0.97	1.00	0.91	1.00	1.03	0.026
A M2 (obs/mod)	0.024-0.028	1.01	1.02	0.96	0.97	0.87	1.00	1.04	0.038
	0.026	0.94	0.97	0.96	1.00	0.95	1.06	1.06	0.043
	0.026-0.027	0.94	0.97	0.96	1.00	0.95	1.08	1.08	0.047
	0.026-0.025	0.94	0.97	0.96	1.01	0.96	1.06	1.05	0.039
	0.027-0.026	0.94	0.98	0.97	1.03	0.98	1.08	1.08	0.046
	0.025-0.026	0.94	0.97	0.95	0.98	0.93	1.05	1.04	0.045
	0.027-0.025	0.94	0.98	0.97	1.03	0.98	1.07	1.06	0.042
	0.025-0.027	0.94	0.97	0.95	0.98	0.92	1.06	1.06	0.051
A K1 (obs/mod)	0.024-0.028	0.94	0.96	0.94	0.96	0.90	1.05	1.06	0.060
	0.026	0.48	3.90	1.27	0.96	0.88	0.56	0.75	0.65
	0.026-0.027	0.48	3.99	1.30	0.96	0.87	0.57	0.76	0.66
	0.026-0.025	0.48	3.80	1.25	0.96	0.88	0.55	0.73	0.64
	0.027-0.026	0.49	3.73	1.23	0.96	0.88	0.57	0.76	0.61
	0.025-0.026	0.47	4.03	1.32	0.97	0.87	0.55	0.73	0.68
	0.027-0.025	0.49	3.62	1.21	0.96	0.89	0.56	0.75	0.60
	0.025-0.027	0.47	4.09	1.35	0.97	0.87	0.56	0.75	0.69
A M4 (obs/mod)	0.024-0.028	0.46	4.12	1.45	0.98	0.87	0.56	0.75	0.71

Table S2. Model evaluation of the model with uniform roughness (n_{man}=0.026) and with dune adjusted roughness. The models are evaluated with the Root Mean Square Error (RMSE) of the observed and modelled water level (h), the correlation coefficient R^2 between the observed and modelled water level (h), and the difference in observed and modelled tidal amplitude (Aζ) of the M2, K1 and M4 tidal constituents (observed divided by modelled values). *the mean of the absolute values of Aζ - 1

	Roughness model	Point Atkinson	Steveston Harbour	Deas Island Tunnel	New Westminster	Port Mann Pumping St	Whonock	Mission	Mean all stations
RMSE h (m)	constant	0.34	0.36	0.42	0.43	0.38	0.31	0.27	0.36
	dune	0.34	0.36	0.34	0.44	0.37	0.31	0.27	0.35
R-squared h	constant	0.87	0.84	0.85	0.74	0.74	0.67	0.72	0.78
	dune	0.87	0.85	0.85	0.75	0.76	0.66	0.7	0.78
Aζ M2 (obs/mod)	constant	1.01	1.03	0.99	1.04	0.95	1.00	1.03	0.03*
	dune	1.00	1.00	0.96	1.00	0.92	1.04	1.08	0.04*
Aζ K1 (obs/mod)	constant	0.94	0.97	0.96	1.00	0.95	1.06	1.06	0.04*
	dune	0.94	0.96	0.95	0.99	0.93	1.09	1.09	0.06*
Aζ M4 (obs/mod)	constant	0.48	3.9	1.27	0.96	0.88	0.56	0.75	0.65*
	dune	0.46	3.89	1.47	0.97	0.88	0.57	0.78	0.67*

Table S3. Statistics (mean, *median in parenthesis), Root Mean Square Error (RMSE)) of the measured and predicted dune height (based on the uniform roughness model with n=0.026 s $m^{-1/3}$ and the predictor of Van Rijn (1984)) for the three focus zones and the total study area.

Δ (m)		**Zone 1**	**Zone 2**	**Zone 3**	**Whole area**
Measured		0.42 (0.39)	0.74 (0.73)	0.37 (0.36)	0.49 (0.44)
Predicted with tidally-averaged shear stress	Mean*	0.80 (0.78)	0.29 (0.27)	0.42 (0.46)	0.44 (0.47)
	RMSE	0.42	0.55	0.29	0.41
Predicted with maximum shear stress	Mean*	0.28 (0.30)	0.73 (0.76)	0.84 (0.85)	0.66 (0.65)
	RMSE	0.27	0.32	0.58	0.41

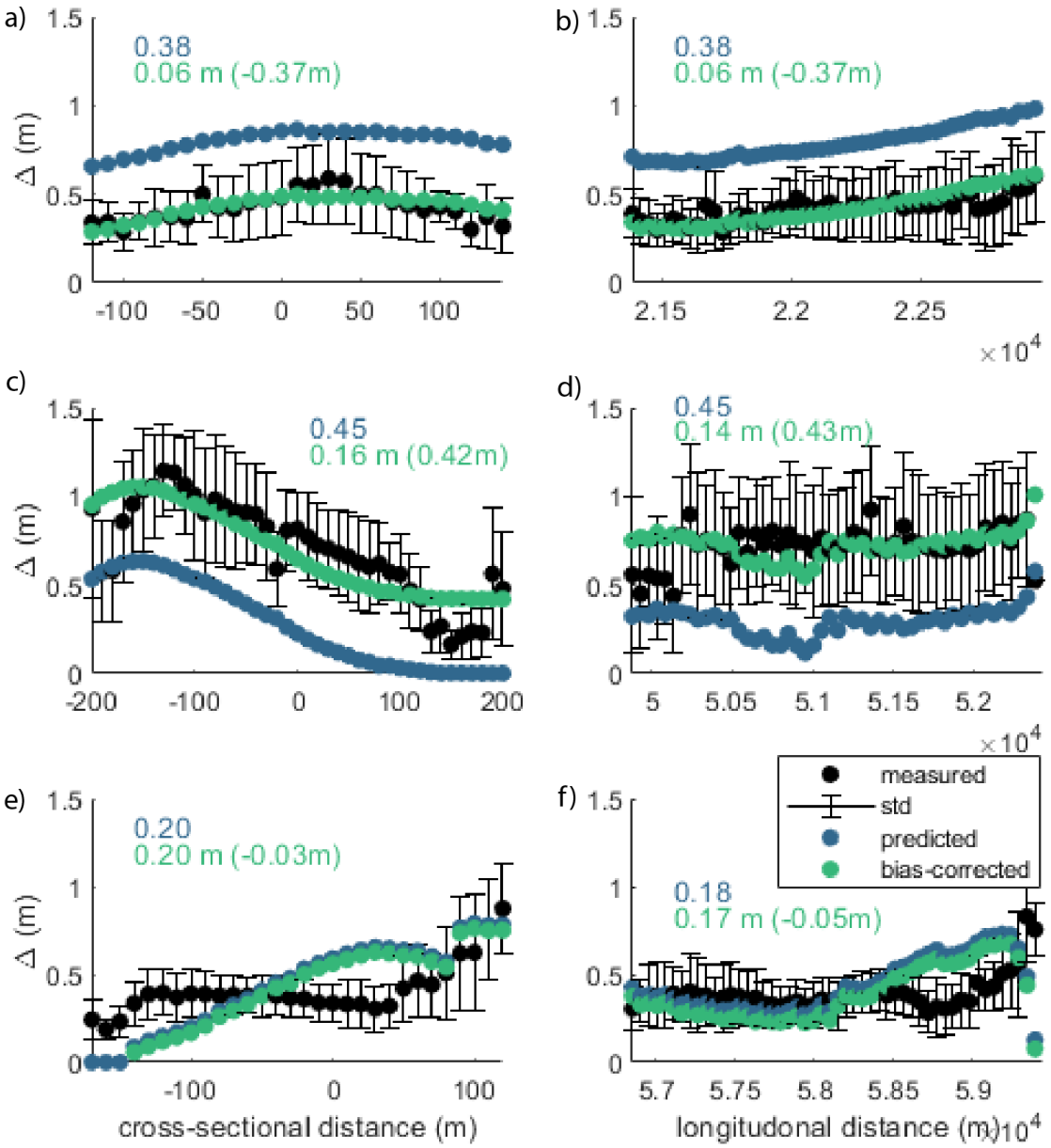

Figure S5. Predicted dune height compared to the measured dune height over the cross-section (a, c, e) and along the river (b, d, f). Dune height is predicted with equation 2 in main manuscript. The RMSE between the predicted and measured dune height is indicated as numbers in the sub-figures. Bias correction is performed to reduce the RMSE and compare the patterns of predicted and measured dune height. In parenthesis the amount of bias correction is shown.

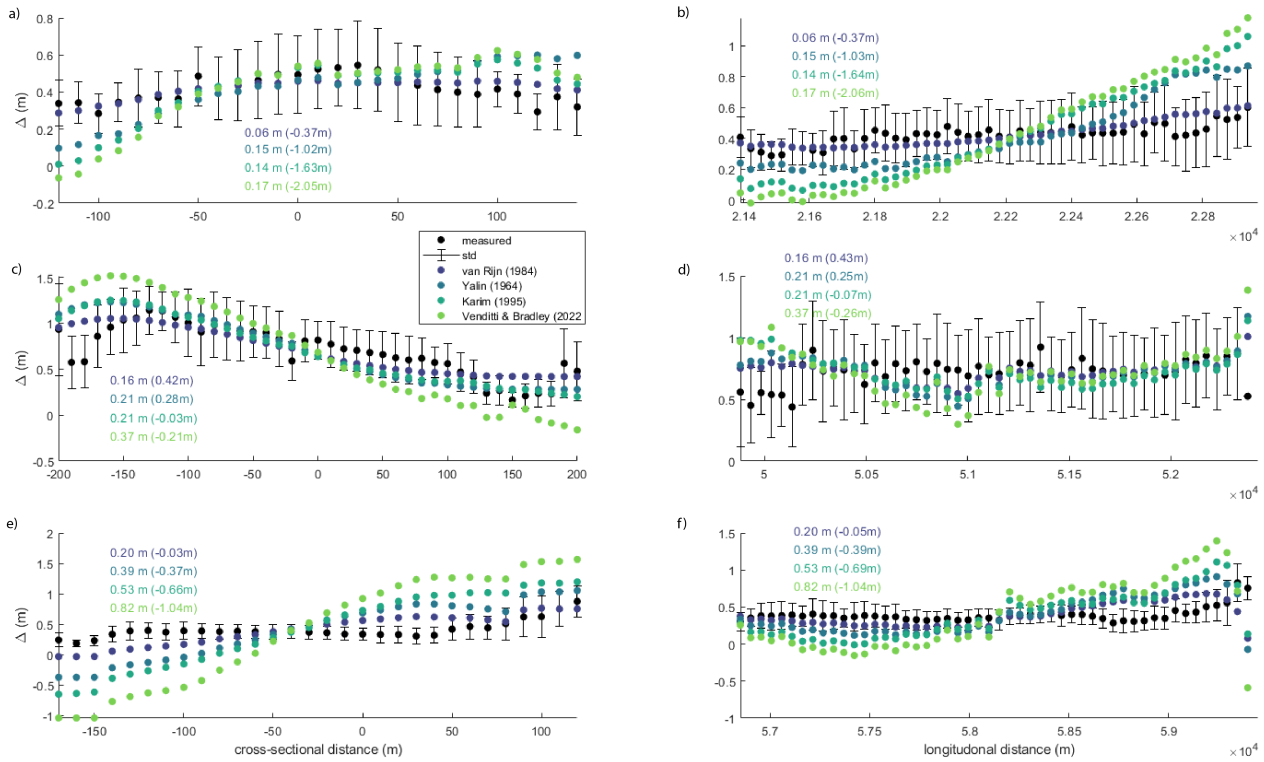

Figure S6. Predicted dune height compared to the measured dune height over the cross-section (a, c, e) and along the river (b, d, f). Dune height is predicted with equation 2, 9, 10 and 12, all in the main manuscript. The RMSE between the bias-corrected predicted and measured dune height is indicated as numbers in the sub-figures. Bias correction is performed to reduce the RMSE and compare the patterns of predicted and measured dune height. In parenthesis the amount of bias correction is shown.

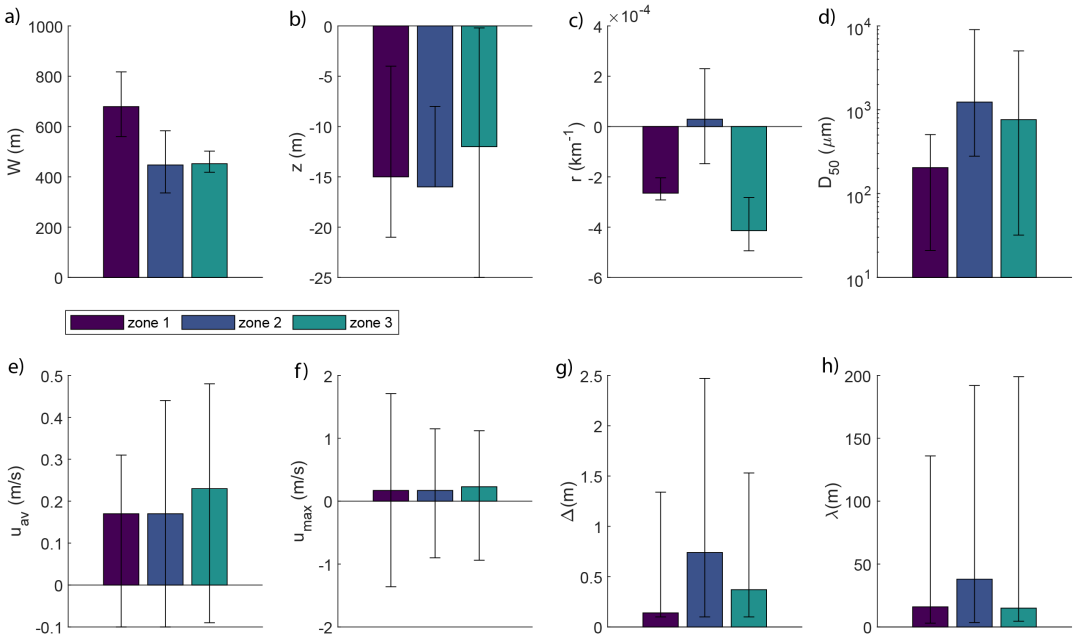

Figure S7. Characteristics of the focus areas. a) width (W), b) bed level (z), c) curvature (r), d) median grain size (D_{50}), e) tidally-averaged flow velocity (u_{av}), f) maximum flow velocity (u_{max}), g) dune height (Δ), h) dune length (λ).

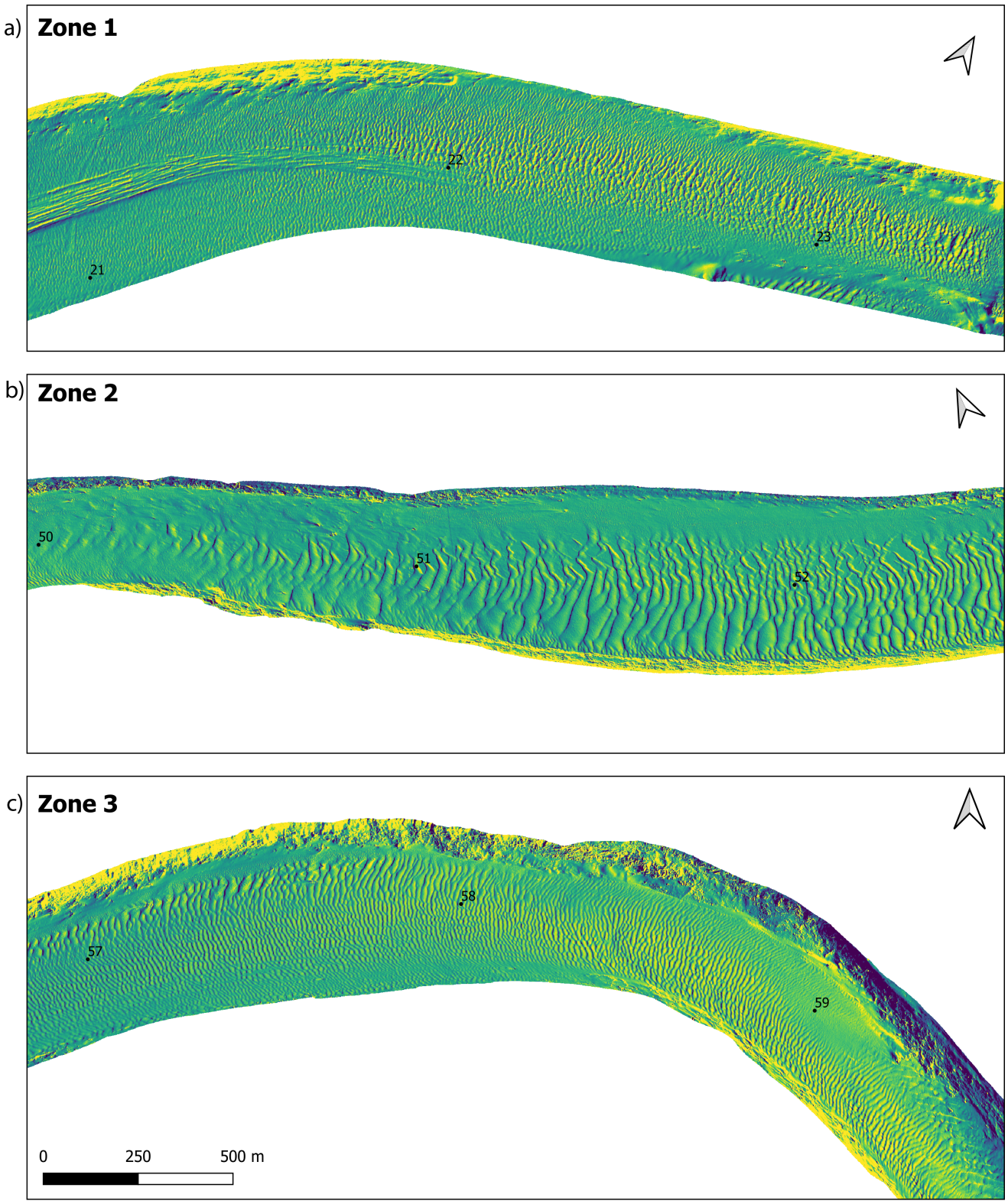

Figure S8. Dune fields in focus areas.

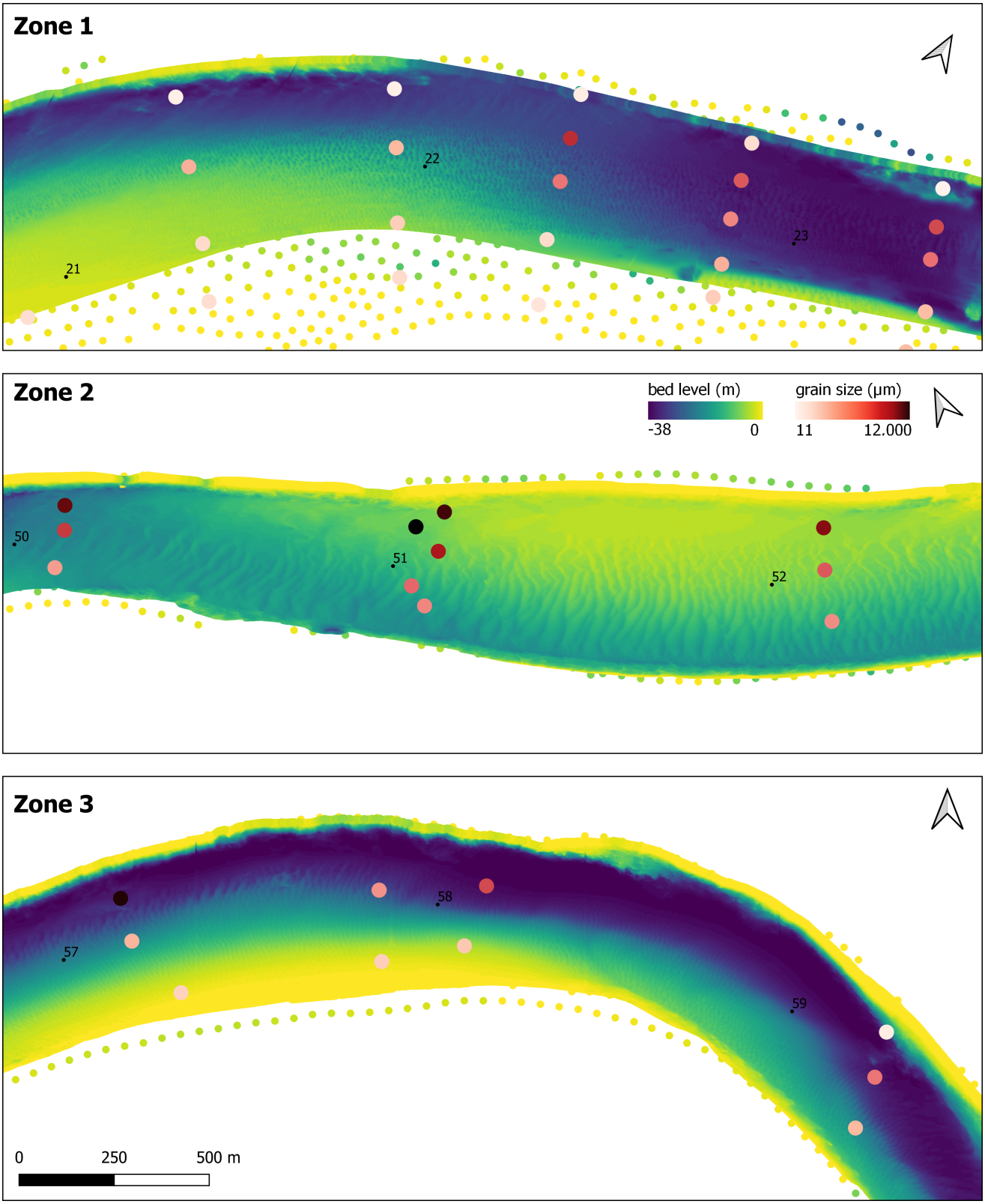

Figure S9. Bed level and grain size (D_{50}) in focus areas.

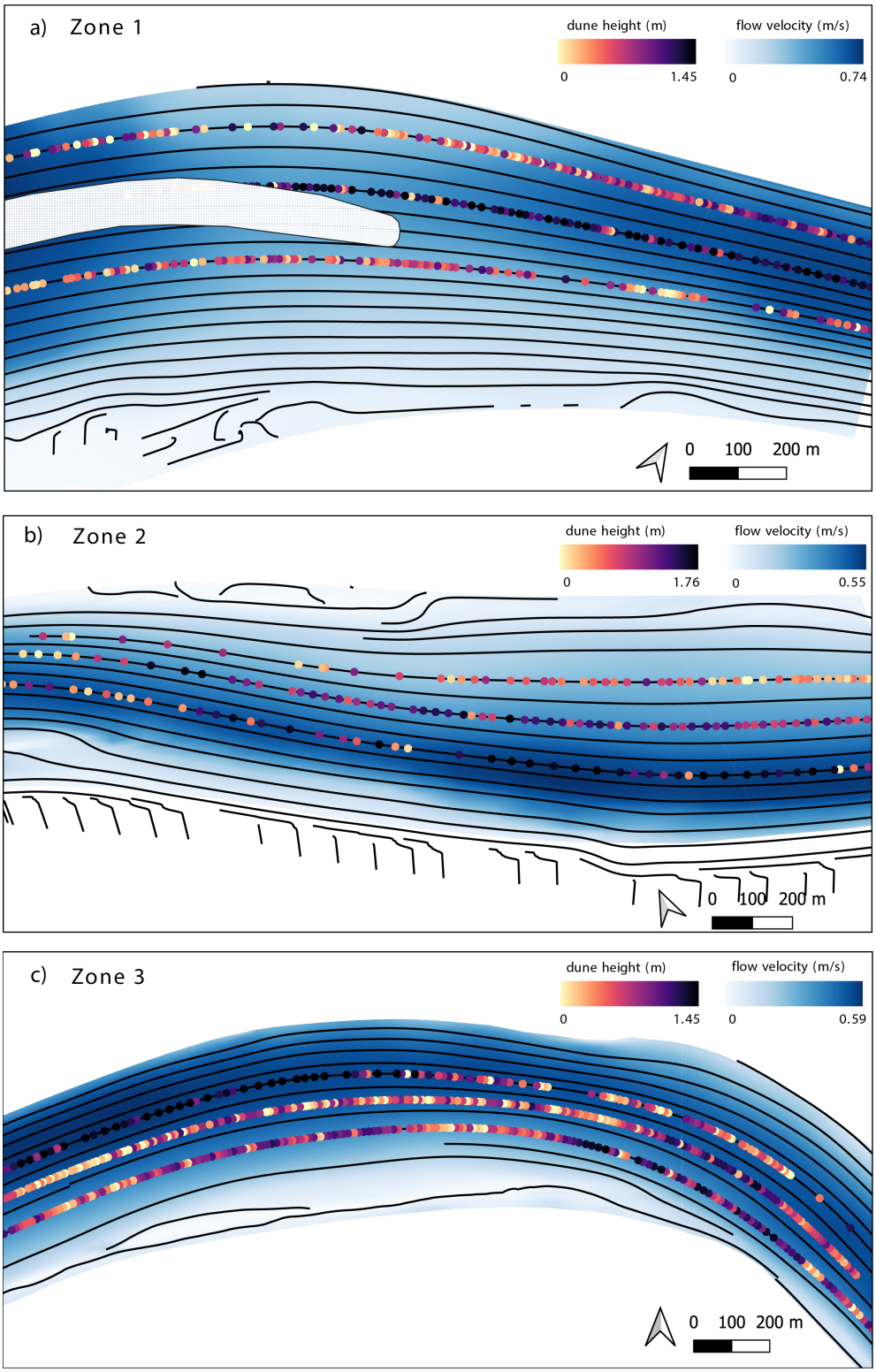

Figure S10. Tidally-averaged flow velocity (blue) in focus areas. Stream lines are indicated in black. Dune height along three the steam lines is shown.

Figure S11. Intertidal areas between Steveston Harbour and Deas Island Tunnel (a), and New Westminster and Port Mann Pumping Station (b). Intertidal areas are shaded in blue.